

Measurement of Direct Photons in Au+Au Collisions at $\sqrt{s_{NN}} = 200$ GeV

S. Afanasiev,¹⁸ C. Aidala,⁷ N.N. Ajitanand,⁴³ Y. Akiba,^{37,38} A. Al-Jamel,³³ J. Alexander,⁴³ K. Aoki,^{23,37} L. Aphecetche,⁴⁵ R. Armendariz,³³ S.H. Aronson,³ R. Averbeck,⁴⁴ T.C. Awes,³⁴ B. Azmoun,³ V. Babintsev,¹⁴ A. Baldisseri,⁸ K.N. Barish,⁴ P.D. Barnes,^{26,*} B. Bassalleck,³² S. Bathe,⁴ S. Batsouli,⁷ V. Baublis,³⁶ F. Bauer,⁴ A. Bazilevsky,³ S. Belikov,^{3,17,*} R. Bennett,⁴⁴ Y. Berdnikov,⁴⁰ M.T. Bjornald,⁷ J.G. Boissevain,²⁶ H. Borel,⁸ K. Boyle,⁴⁴ M.L. Brooks,²⁶ D.S. Brown,³³ D. Bucher,²⁹ H. Buesching,³ V. Bumazhnov,¹⁴ G. Bunce,^{3,38} J.M. Burward-Hoy,²⁶ S. Butsyk,⁴⁴ S. Campbell,⁴⁴ J.-S. Chai,¹⁹ S. Chernichenko,¹⁴ C.Y. Chi,⁷ J. Chiba,²⁰ M. Chiu,⁷ I.J. Choi,⁵³ T. Chujo,⁴⁹ V. Cianciolo,³⁴ C.R. Clevon,¹² Y. Cobigo,⁸ B.A. Cole,⁷ M.P. Comets,³⁵ M. Connors,⁴⁴ P. Constantin,¹⁷ M. Csanád,¹⁰ T. Csörgő,⁵² T. Dahms,⁴⁴ K. Das,¹¹ G. David,³ H. Delagrange,⁴⁵ A. Denisov,¹⁴ D. d'Enterria,⁷ A. Deshpande,^{38,44} E.J. Desmond,³ O. Dietzsch,⁴¹ A. Dion,⁴⁴ J.L. Drachenberg,¹ O. Drapier,²⁴ A. Drees,⁴⁴ A.K. Dubey,⁵¹ A. Durum,¹⁴ V. Dzhordzhadze,⁴⁶ Y.V. Efremenko,³⁴ J. Egdemir,⁴⁴ A. Enokizono,¹³ H. En'yo,^{37,38} B. Espagnon,³⁵ S. Esumi,⁴⁸ D.E. Fields,^{32,38} F. Fleuret,²⁴ S.L. Fokin,²² B. Forestier,²⁷ Z. Fraenkel,^{51,*} J.E. Frantz,⁷ A. Franz,³ A.D. Frawley,¹¹ Y. Fukao,^{23,37} S.-Y. Fung,⁴ S. Gadrat,²⁷ F. Gastineau,⁴⁵ M. Germain,⁴⁵ A. Glenn,⁴⁶ M. Gonin,²⁴ J. Gosset,⁸ Y. Goto,^{37,38} R. Granier de Cassagnac,²⁴ N. Grau,¹⁷ S.V. Greene,⁴⁹ M. Grosse Perdekamp,^{15,38} T. Gunji,⁵ H.-Å. Gustafsson,^{28,*} T. Hachiya,^{13,37} A. Hadj Henni,⁴⁵ J.S. Haggerty,³ M.N. Hagiwara,¹ H. Hamagaki,⁵ H. Harada,¹³ E.P. Hartouni,²⁵ K. Haruna,¹³ M. Harvey,³ E. Haslum,²⁸ K. Hasuko,³⁷ R. Hayano,⁵ X. He,¹² M. Heffner,²⁵ T.K. Hemmick,⁴⁴ J.M. Heuser,³⁷ H. Hiejima,¹⁵ J.C. Hill,¹⁷ R. Hobbs,³² M. Holmes,⁴⁹ W. Holzmann,⁴³ K. Homma,¹³ B. Hong,²¹ T. Horaguchi,^{37,47} M.G. Hur,¹⁹ T. Ichihara,^{37,38} H. Iinuma,^{23,37} K. Imai,^{23,37} J. Imrek,⁹ M. Inaba,⁴⁸ D. Isenhower,¹ L. Isenhower,¹ M. Ishihara,³⁷ T. Isobe,⁵ M. Issah,⁴³ A. Isupov,¹⁸ B.V. Jacak,^{44,†} J. Jia,⁷ J. Jin,⁷ O. Jinnouchi,³⁸ B.M. Johnson,³ K.S. Joo,³⁰ D. Jouan,³⁵ F. Kajihara,^{5,37} S. Kametani,^{5,50} N. Kamihara,^{37,47} M. Kaneta,³⁸ J.H. Kang,⁵³ T. Kawagishi,⁴⁸ A.V. Kazantsev,²² S. Kelly,⁶ A. Khanzadeev,³⁶ D.J. Kim,⁵³ E. Kim,⁴² Y.-S. Kim,¹⁹ E. Kinney,⁶ Á. Kiss,¹⁰ E. Kistenev,³ A. Kiyomichi,³⁷ C. Klein-Boesing,²⁹ L. Kochenda,³⁶ V. Kochetkov,¹⁴ B. Komkov,³⁶ M. Konno,⁴⁸ D. Kotchetkov,⁴ A. Kozlov,⁵¹ P.J. Kroon,³ G.J. Kunde,²⁶ N. Kurihara,⁵ K. Kurita,^{37,39} M.J. Kweon,²¹ Y. Kwon,⁵³ G.S. Kyle,³³ R. Lacey,⁴³ J.G. Lajoie,¹⁷ A. Lebedev,¹⁷ Y. Le Bornec,³⁵ S. Leckey,⁴⁴ D.M. Lee,²⁶ M.K. Lee,⁵³ M.J. Leitch,²⁶ M.A.L. Leite,⁴¹ X.H. Li,⁴ H. Lim,⁴² A. Litvinenko,¹⁸ M.X. Liu,²⁶ C.F. Maguire,⁴⁹ Y.I. Makdisi,³ A. Malakhov,¹⁸ M.D. Malik,³² V.I. Manko,²² H. Masui,⁴⁸ F. Matathias,⁴⁴ M.C. McCain,¹⁵ P.L. McGaughey,²⁶ Y. Miake,⁴⁸ T.E. Miller,⁴⁹ A. Milov,⁴⁴ S. Mioduszewski,³ G.C. Mishra,¹² J.T. Mitchell,³ D.P. Morrison,³ J.M. Moss,²⁶ T.V. Moukhanova,²² D. Mukhopadhyay,⁴⁹ J. Murata,^{37,39} S. Nagamiya,²⁰ Y. Nagata,⁴⁸ J.L. Nagle,⁶ M. Naglis,⁵¹ T. Nakamura,¹³ J. Newby,²⁵ M. Nguyen,⁴⁴ B.E. Norman,²⁶ A.S. Nyanin,²² J. Nystrand,²⁸ E. O'Brien,³ C.A. Ogilvie,¹⁷ H. Ohnishi,³⁷ I.D. Ojha,⁴⁹ K. Okada,³⁸ O.O. Omiwade,¹ A. Oskarsson,²⁸ I. Otterlund,²⁸ K. Ozawa,⁵ D. Pal,⁴⁹ A.P.T. Palounek,²⁶ V. Pantuev,^{16,44} V. Papavassiliou,³³ J. Park,⁴² W.J. Park,²¹ S.F. Pate,³³ H. Pei,¹⁷ J.-C. Peng,¹⁵ H. Pereira,⁸ V. Peresedov,¹⁸ D.Yu. Peressounko,²² C. Pinkenburg,³ R.P. Pisani,³ M.L. Purschke,³ A.K. Purwar,⁴⁴ H. Qu,¹² J. Rak,¹⁷ I. Ravinovich,⁵¹ K.F. Read,^{34,46} M. Reuter,⁴⁴ K. Reygers,²⁹ V. Riabov,³⁶ Y. Riabov,³⁶ G. Roche,²⁷ A. Romana,^{24,*} M. Rosati,¹⁷ S.S.E. Rosendahl,²⁸ P. Rosnet,²⁷ P. Rukoyatkin,¹⁸ V.L. Rykov,³⁷ S.S. Ryu,⁵³ B. Sahlmueller,^{29,44} N. Saito,^{23,37,38} T. Sakaguchi,^{5,50} S. Sakai,⁴⁸ V. Samsonov,³⁶ H.D. Sato,^{23,37} S. Sato,^{3,20,48} S. Sawada,²⁰ V. Semenov,¹⁴ R. Seto,⁴ D. Sharma,⁵¹ T.K. Shea,³ I. Shein,¹⁴ T.-A. Shibata,^{37,47} K. Shigaki,¹³ M. Shimomura,⁴⁸ T. Shohjoh,⁴⁸ K. Shoji,^{23,37} A. Sickles,⁴⁴ C.L. Silva,⁴¹ D. Silvermyr,³⁴ K.S. Sim,²¹ C.P. Singh,² V. Singh,² S. Skutnik,¹⁷ W.C. Smith,¹ A. Soldatov,¹⁴ R.A. Soltz,²⁵ W.E. Sondheim,²⁶ S.P. Sorensen,⁴⁶ I.V. Sourikova,³ F. Staley,⁸ P.W. Stankus,³⁴ E. Stenlund,²⁸ M. Stepanov,³³ A. Ster,⁵² S.P. Stoll,³ T. Sugitate,¹³ C. Suire,³⁵ J.P. Sullivan,²⁶ J. Sziklai,⁵² T. Tabaru,³⁸ S. Takagi,⁴⁸ E.M. Takagui,⁴¹ A. Taketani,^{37,38} K.H. Tanaka,²⁰ Y. Tanaka,³¹ K. Tanida,^{37,38,42} M.J. Tannenbaum,³ A. Taranenko,⁴³ P. Tarján,⁹ T.L. Thomas,³² M. Togawa,^{23,37} J. Tojo,³⁷ H. Torii,³⁷ R.S. Towell,¹ V.-N. Tram,²⁴ I. Tserruya,⁵¹ Y. Tsuchimoto,^{13,37} S.K. Tuli,^{2,*} H. Tydesjö,²⁸ N. Tyurin,¹⁴ C. Vale,¹⁷ H. Valle,⁴⁹ H.W. van Hecke,²⁶ J. Velkovska,⁴⁹ R. Vértesi,⁹ A.A. Vinogradov,²² E. Vznuzdaev,³⁶ M. Wagner,^{23,37} X.R. Wang,³³ Y. Watanabe,^{37,38} J. Wessels,²⁹ S.N. White,³ N. Willis,³⁵ D. Winter,⁷ C.L. Woody,³ M. Wysocki,⁶ W. Xie,^{4,38} A. Yanovich,¹⁴ S. Yokkaichi,^{37,38} G.R. Young,³⁴ I. Younus,³² I.E. Yushmanov,²² W.A. Zajc,⁷ O. Zaudtke,²⁹ C. Zhang,⁷ J. Zimányi,^{52,*} and L. Zolin¹⁸

(PHENIX Collaboration)

¹Abilene Christian University, Abilene, Texas 79699, USA

²Department of Physics, Banaras Hindu University, Varanasi 221005, India

- ³Brookhaven National Laboratory, Upton, New York 11973-5000, USA
⁴University of California - Riverside, Riverside, California 92521, USA
⁵Center for Nuclear Study, Graduate School of Science, University of Tokyo, 7-3-1 Hongo, Bunkyo, Tokyo 113-0033, Japan
⁶University of Colorado, Boulder, Colorado 80309, USA
⁷Columbia University, New York, New York 10027 and Nevis Laboratories, Irvington, New York 10533, USA
⁸Dapnia, CEA Saclay, F-91191, Gif-sur-Yvette, France
⁹Debrecen University, H-4010 Debrecen, Egyetem tér 1, Hungary
¹⁰ELTE, Eötvös Loránd University, H - 1117 Budapest, Pázmány P. s. 1/A, Hungary
¹¹Florida State University, Tallahassee, Florida 32306, USA
¹²Georgia State University, Atlanta, Georgia 30303, USA
¹³Hiroshima University, Kagamiyama, Higashi-Hiroshima 739-8526, Japan
¹⁴IHEP Protvino, State Research Center of Russian Federation, Institute for High Energy Physics, Protvino, 142281, Russia
¹⁵University of Illinois at Urbana-Champaign, Urbana, Illinois 61801, USA
¹⁶Institute for Nuclear Research of the Russian Academy of Sciences, prospekt 60-letiya Oktyabrya 7a, Moscow 117312, Russia
¹⁷Iowa State University, Ames, Iowa 50011, USA
¹⁸Joint Institute for Nuclear Research, 141980 Dubna, Moscow Region, Russia
¹⁹KAERI, Cyclotron Application Laboratory, Seoul, Korea
²⁰KEK, High Energy Accelerator Research Organization, Tsukuba, Ibaraki 305-0801, Japan
²¹Korea University, Seoul, 136-701, Korea
²²Russian Research Center “Kurchatov Institute”, Moscow, 123098 Russia
²³Kyoto University, Kyoto 606-8502, Japan
²⁴Laboratoire Leprince-Ringuet, Ecole Polytechnique, CNRS-IN2P3, Route de Saclay, F-91128, Palaiseau, France
²⁵Lawrence Livermore National Laboratory, Livermore, California 94550, USA
²⁶Los Alamos National Laboratory, Los Alamos, New Mexico 87545, USA
²⁷LPC, Université Blaise Pascal, CNRS-IN2P3, Clermont-Fd, 63177 Aubiere Cedex, France
²⁸Department of Physics, Lund University, Box 118, SE-221 00 Lund, Sweden
²⁹Institut für Kernphysik, University of Muenster, D-48149 Muenster, Germany
³⁰Myongji University, Yongin, Kyonggido 449-728, Korea
³¹Nagasaki Institute of Applied Science, Nagasaki-shi, Nagasaki 851-0193, Japan
³²University of New Mexico, Albuquerque, New Mexico 87131, USA
³³New Mexico State University, Las Cruces, New Mexico 88003, USA
³⁴Oak Ridge National Laboratory, Oak Ridge, Tennessee 37831, USA
³⁵IPN-Orsay, Université Paris Sud, CNRS-IN2P3, BP1, F-91406, Orsay, France
³⁶PNPI, Petersburg Nuclear Physics Institute, Gatchina, Leningrad region, 188300, Russia
³⁷RIKEN Nishina Center for Accelerator-Based Science, Wako, Saitama 351-0198, Japan
³⁸RIKEN BNL Research Center, Brookhaven National Laboratory, Upton, New York 11973-5000, USA
³⁹Physics Department, Rikkyo University, 3-34-1 Nishi-Ikebukuro, Toshima, Tokyo 171-8501, Japan
⁴⁰Saint Petersburg State Polytechnic University, St. Petersburg, 195251 Russia
⁴¹Universidade de São Paulo, Instituto de Física, Caixa Postal 66318, São Paulo CEP05315-970, Brazil
⁴²Seoul National University, Seoul, Korea
⁴³Chemistry Department, Stony Brook University, SUNY, Stony Brook, New York 11794-3400, USA
⁴⁴Department of Physics and Astronomy, Stony Brook University, SUNY, Stony Brook, New York 11794-3400, USA
⁴⁵SUBATECH (Ecole des Mines de Nantes, CNRS-IN2P3, Université de Nantes) BP 20722 - 44307, Nantes, France
⁴⁶University of Tennessee, Knoxville, Tennessee 37996, USA
⁴⁷Department of Physics, Tokyo Institute of Technology, Oh-okayama, Meguro, Tokyo 152-8551, Japan
⁴⁸Institute of Physics, University of Tsukuba, Tsukuba, Ibaraki 305, Japan
⁴⁹Vanderbilt University, Nashville, Tennessee 37235, USA
⁵⁰Waseda University, Advanced Research Institute for Science and Engineering, 17 Kikui-cho, Shinjuku-ku, Tokyo 162-0044, Japan
⁵¹Weizmann Institute, Rehovot 76100, Israel
⁵²Institute for Particle and Nuclear Physics, Wigner Research Centre for Physics, Hungarian Academy of Sciences (Wigner RCP, RMKI) H-1525 Budapest 114, POBox 49, Budapest, Hungary
⁵³Yonsei University, IPAP, Seoul 120-749, Korea

(Dated: May 28, 2012)

We report the measurement of direct photons at midrapidity in Au+Au collisions at $\sqrt{s_{NN}} = 200$ GeV. The direct photon signal was extracted for the transverse momentum range of $4 \text{ GeV}/c < p_T < 22 \text{ GeV}/c$, using a statistical method to subtract decay photons from the inclusive photon sample. The direct-photon nuclear-modification factor R_{AA} was calculated as a function of p_T for different Au+Au collision centralities using the measured $p+p$ direct-photon spectrum and compared to theoretical predictions. R_{AA} was found to be consistent with unity for all centralities over the entire measured p_T range. Theoretical models that account for modifications of initial-direct-photon production due to modified-parton-distribution functions (PDFs) in Au and the different isospin composition of the nuclei predict a modest change of R_{AA} from unity. They are consistent with

the data. Models with compensating effects of the quark-gluon plasma on high-energy photons, such as suppression of jet-fragmentation photons and induced-photon bremsstrahlung from partons traversing the medium, are also consistent with this measurement.

PACS numbers: 25.75.Dw

Direct photons are a powerful probe to study ultra-relativistic heavy-ion collisions where a hot and dense quark-gluon plasma (QGP) is formed. Direct photons are defined as all photons that arise from processes during the collision, rather than from decays of hadrons. The biggest challenge in the measurement of direct photons is to distinguish them from the large background of decay photons.

Direct photons with intermediate and high transverse momentum ($p_T > 4$ GeV/ c) are produced predominantly from initial-hard-scattering processes of the colliding quarks or gluons, such as $q+g \rightarrow q+\gamma$ or $q+\bar{q} \rightarrow g+\gamma$. In addition, they can be produced as bremsstrahlung emitted by a scattered parton, from the fragmentation of quarks and gluons, or from the interaction of a scattered parton with the medium created in heavy-ion collisions [1–5]. Additional photons may be emitted at low transverse momentum as thermal radiation from the partonic and hadronic phases.

The production of direct photons, if compared to the scaled $p+p$ rates, is also affected by possible modifications of the initial state of the colliding nuclei, like shadowing and anti-shadowing, and by the different isospin composition of Au nuclei in contrast to protons, as explained in Sec. 2.2 of [6]. In addition, the different quark charge squared content of p and n influences the yields from initial hard scattering in heavy ions, as explained in detail in Sec. 3.3 of [6].

The direct photons should not be affected by the medium as they traverse it, since they are both electrically and color neutral, but the presence of the medium can affect the total direct photon yield. For instance, parton energy loss [7–9] can reduce the fraction of fragmentation photons at a given p_T , while the scattering of a hard parton on a thermal one can produce a high p_T photon with approximately the same momentum as the original parton (jet-photon conversion) [1]. As a result, theoretical models predict that the yield of direct photons in Au+Au collisions will be somewhat modified compared to the scaled yield from $p+p$ collisions at the same energy [2–5].

Previous PHENIX measurements of direct photon spectra in Au+Au at $\sqrt{s_{NN}} = 200$ GeV, from the 2002 RHIC run, showed no significant deviation above $p_T > 6$ GeV/ c from the scaled invariant yield of NLO pQCD predictions for $p+p$ collisions [10]. On the other hand, PHENIX measurements of virtual direct photons at low transverse momentum ($p_T < 4$ GeV/ c) found a large exponentially distributed excess of direct photons, compared to the scaled $p+p$ QCD prediction, which was

attributed to thermal photon radiation from the QGP formed in central Au+Au collisions [11]. Although the contribution of thermal photons at large p_T quickly diminishes due to the exponential falloff, the direct photon yield at high p_T may be modified in nuclear collisions due to the various effects mentioned above and deserves careful study.

We report on the measurement of direct photons in Au+Au collisions at $\sqrt{s_{NN}} = 200$ GeV at RHIC from data taken by the PHENIX experiment [12] in 2004. The analysis used 1.03×10^9 minimum bias events, which is more than a tenfold increase compared to the previous measurement [10]. The centrality (impact parameter) of the Au+Au collision was determined from the correlation between the number of charged particles detected in the Beam-Beam Counters (BBC), in the pseudorapidity range $3.0 < |\eta| < 3.9$, and the energy measured in the zero-degree calorimeters (ZDC). The average number of binary nucleon-nucleon collisions ($\langle N_{\text{coll}} \rangle$) was estimated for each centrality bin with a Glauber Model Monte Carlo that simulated the BBC and ZDC responses [13].

Photon candidates were reconstructed in the electromagnetic calorimeter (EMCal) located in the central arms of PHENIX [14]. The EMCal covers $|\eta| < 0.35$. It comprises six sectors of lead-scintillator calorimeter (PbSc) and two sectors of lead-glass Čerenkov calorimeter (PbGl). Located at a radial distance of about 5 m, the two subsystems cover a total of π in azimuth. The segmentation is $\Delta\phi \times \Delta\eta \sim 0.011 \times 0.011$ for PbSc and $\sim 0.008 \times 0.008$ for PbGl.

At high transverse momenta, the minimum opening angle between the two photons of a π^0 decay decreases, and the distance between the two clusters on the EMCal surface becomes comparable to the tower segmentation, with the result that the showers begin to merge. This starts to occur at ~ 10 GeV/ c (16 GeV/ c), and affects 50% of all π^0 decays at $p_T \sim 16$ GeV/ c (24 GeV/ c) for the PbSc (PbGl) detector. Furthermore, when the decay photons partially overlap, but are not yet indistinguishably merged, the energy may be imperfectly shared by the clustering algorithm: one reconstructed cluster has more, the other has less energy than the original photons. This may change the apparent photon yield, particularly at high p_T . The effect is significant for the PbSc, but negligible for the PbGl in the measured p_T range.

Direct photons were measured on a statistical basis, as in earlier PHENIX direct photon measurements [10, 15]. Photon-like clusters were identified by applying Particle Identification (PID) cuts based on the parameterized shower profile for a photon. The analyses were performed

independently with the PbSc and the PbGl calorimeters, and the fully corrected results were combined. Since the methods were different for the two detectors, the systematic uncertainties are uncorrelated.

In the analysis of the PbGl data, the $\approx 10 - 15\%$ contamination of the photon candidate spectra with charged particles was subtracted by associating photon candidates with charged hits in the pad chamber (PC3) situated directly in front of the calorimeter. Neutrons and anti-neutrons (5% contribution to the cluster energy spectrum at 4 GeV, vanishing at 7 GeV) were subtracted based on a full GEANT [16] simulation of the detector response.

The spectra were also corrected for the loss of photons due to conversions into e^+e^- pairs in the material in front of the PbGl. The resulting spectra were corrected for the detector acceptance and reconstruction efficiency. The acceptance is influenced by the detector geometry and the exclusion of detector areas from the analysis. It was calculated with a Monte Carlo simulation. The efficiency correction takes into account the energy resolution of the calorimeter, the applied PID cuts, and occupancy effects in the high-multiplicity environment. The reconstruction efficiency was determined by embedding simulated photons into real events and analyzing these embedded photons with the same analysis cuts.

Merged clusters at high p_T were removed by the PID cuts. Photons from hadron decays, mainly from π^0 and η , measured by PHENIX [17, 18], were simulated using the decay kinematics and detector geometry and, following the method used in earlier analyses [10], used to calculate the ratio $R_\gamma = \frac{\gamma_{inclusive}^{data}/\pi^0_{data}}{\gamma_{decay}^{MC}/\pi^0_{MC}} = \frac{\gamma_{inclusive}^{data}}{\gamma_{decay}^{MC}}$. This ratio was used to extract the direct photon invariant yield via $\gamma_{direct} = (1 - \frac{1}{R_\gamma})\gamma_{inclusive}$.

In the PbSc analysis, photon candidates (clusters passing PID cuts) were corrected for the fraction of electrons, charged hadrons, and neutrons passing those PID cuts; this fraction was derived from full GEANT detector simulations using particle spectra measured by PHENIX. The result was the raw inclusive photon distribution. Note that at higher p_T the calorimeter response to true single photons and correlated decay photons is different, therefore, the raw inclusive spectrum cannot be corrected in one simple step. Instead, first the expected raw distribution of background photons from hadron decays (predominantly π^0 and η), containing all detector effects, denoted $2\gamma_{decay,raw}^{MC}$, was calculated in a full GEANT simulation which used the measured π^0 and η spectra [17, 18]. After subtracting the raw decay photons from the raw inclusive photons, the acceptance and efficiency correction for the remaining direct (single) photons was obtained using simulated single photons embedded in real events. These corrections were then applied to the raw direct single-photon distribution to get the final direct-single-photon distribution γ_{direct}^{data} , the experimental result. The

TABLE I: Statistical and systematic uncertainties of the direct photon yield, in %, for Au+Au minimum bias events, as estimated for the measurement with the PbGl (PbSc). The values for three transverse momenta are given. All systematic uncertainties are correlated in p_T .

Error type / p_T	4.75 GeV/c	9.25 GeV/c	15 GeV/c
Background corrections	9.1 (5.2)	5.7 (2.5)	5.1 (2.2)
Yield corrections	11.9 (10.5)	8.3 (9.4)	7.9 (11.2)
Energy scale	7.9 (6.8)	6.8 (7.0)	6.8 (7.0)
Decay γ simulation	12.5 (7.2)	5.2 (4.3)	3.8 (3.7)
Total Systematic	21.0 (13.9)	13.2 (12.7)	12.3 (13.9)
Total Statistical	0.9 (0.4)	4.1 (2.6)	8.8 (8.2)
Combined Systematic	11.6	9.1	9.3
Combined Statistical	0.4	2.1	5.9

result from the $2\gamma_{decay,raw}^{MC}$ in the PbSc analysis cannot be simply acceptance corrected to get the true decay- γ background, therefore, the ratio R_γ for the PbSc was calculated using the decay photon background Monte Carlo calculation from the PbGl analysis as $R_\gamma = \frac{\gamma_{direct}^{data} + \gamma_{decay}^{MC}}{\gamma_{decay}^{MC}}$.

For both the PbGl and PbSc measurements, there are four distinct sources of systematic uncertainties (Table I), all of which are p_T -correlated. Uncertainties from background corrections come from the subtraction of hadron and electron contamination and corrections for photon conversions. The corrections to the raw yields by the simulations are another source of uncertainty. The energy scale of the calorimeters is only known with a 1.2% precision and thus leads to uncertainties in the direct photon measurement. The decay photon calculation adds further systematic uncertainties due to the extraction of the π^0 [17], the parameterization of the input hadron spectra and ratios such as η/π^0 .

The fully corrected results obtained with the two analyses agree within their respective uncertainties and were combined. The spectra and nuclear modification factors in this publication represent a weighted average of the two independent measurements. Since the systematic uncertainties are taken to be uncorrelated between the two analyses, the weight w was determined from their total uncertainty σ_{Total} , which is the quadratic sum of all statistical and systematic uncertainties, by $w = 1/\sigma_{Total}^2$. [19]

The ratio R_γ is shown in Fig. 1 for minimum bias Au+Au collisions and the two extreme centrality bins. An excess above unity indicates the presence of direct photons. Such an excess is clearly visible for all centrality selections. The ratio R_γ increases with centrality due to the suppression of the π^0 [7, 8] and the associated decay photons.

The combined direct photon spectra in Au+Au colli-

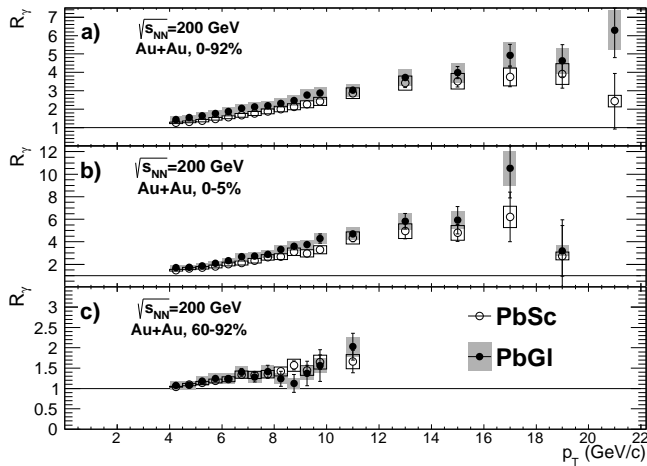


FIG. 1: Ratio R_γ for different centrality selections, for the PbGl and the PbSc analysis. The error bars indicate point-to-point uncertainties, the boxes around the points indicate p_T correlated uncertainties.

sions are shown in the top panel of Fig. 2 for ten centrality selections. The shape of the spectra are seen to be similar for all centralities. The bottom panel shows a comparison of the PbGl and PbSc spectra to the combined result for the 0–5% most central collisions. A good agreement between the two measurements is observed.

Fig. 2 also includes the $p+p$ spectrum at the same energy, measured by PHENIX [20]. The $p+p$ spectrum is compared to a power law fit $(A/p_T)^n$ with power $n = 7.08 \pm 0.09(\text{stat}) \pm 0.1(\text{syst})$ obtained by fitting the region $p_T > 8$ GeV/c [20]. The fit is extrapolated to lower p_T . A power law fit to the minimum bias (most central) Au+Au spectrum yields a power of $n = 6.85 \pm 0.07(\text{stat}) \pm 0.02(\text{syst})$ ($n = 7.18 \pm 0.14(\text{stat}) \pm 0.06(\text{syst})$) consistent with the power of the $p+p$ fit. The agreement indicates no apparent shape modification of the spectra compared to $p+p$ collisions.

For hard processes, the yield in A+A collisions for a particular impact parameter selection is expected to be equal to the cross section in $p+p$ collisions, scaled by the average nuclear thickness function $\langle T_{AA} \rangle = \langle N_{\text{coll}} \rangle / \sigma_{pp}^{\text{inel}}$ for the associated centrality selection. Here, $\langle N_{\text{coll}} \rangle$ is the number of binary nucleon-nucleon collisions, calculated with the Glauber Model Monte Carlo for the selected centrality, and $\sigma_{pp}^{\text{inel}}$ is the total inelastic $p+p$ cross section of 42 mb. In Fig. 2, the power law fit to the $p+p$ direct photon spectrum has been scaled by the nuclear thickness function for each of the ten centrality selections, and overlaid on the measured result for that centrality. The comparison indicates that the magnitude, as well as the shape of the direct photon spectra, are in agreement with expectations from $p+p$ collisions for all centralities.

Nuclear effects are quantified by the nuclear modification factor, R_{AA} . For a given centrality selection, R_{AA} is given by the ratio of the measured invariant yields in

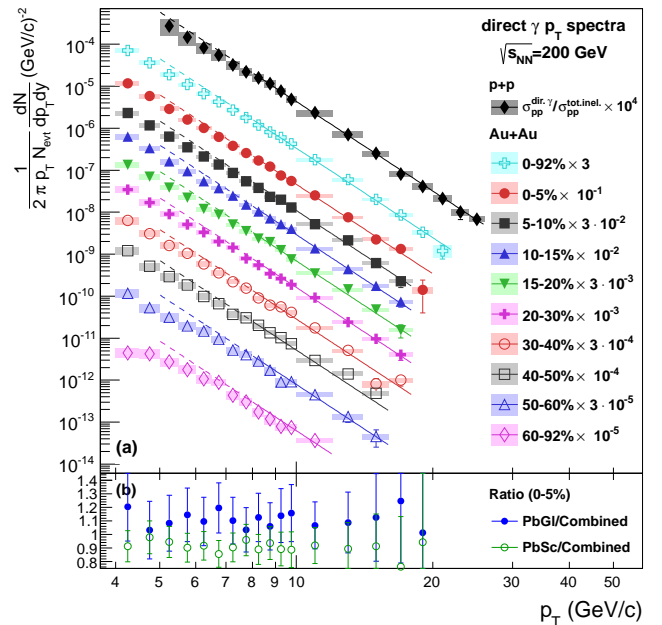


FIG. 2: (a) Direct photon spectra for all centrality selections in Au+Au, and for $p+p$ measured in [20]. The error bars indicate point-to-point uncertainties, the boxes around the points indicate p_T correlated uncertainties. The lines depict a T_{AA} scaled fit for $p_T > 8$ GeV/c to the $p+p$ cross section, they are dashed for the range where the fit is extrapolated to lower p_T . (b) Comparison of the PbGl and PbSc results with the combined result for the 0–5% most central events. The error bars show the total uncertainties.

Au+Au collisions, divided by the production cross section for the same particle in $p+p$ collisions, scaled with the average nuclear thickness function for that centrality:

$$R_{AA}(p_T) = \frac{(1/N_{AA}^{\text{evt}})d^2 N_{AA}/dp_T dy}{\langle T_{AA} \rangle \times d^2 \sigma_{pp}/dp_T dy}, \quad (1)$$

where $d^2 \sigma_{pp}/dp_T dy$ is the measured $p+p$ cross section for direct photons [20].

The direct photon nuclear modification factor is shown in Fig. 3 for three different centrality selections. The R_{AA} results are calculated using the measured direct photon results from $p+p$ collisions for the first time. The R_{AA} values are consistent with unity, within errors, for all centrality selections over the entire p_T range.

In Fig. 4, the measured nuclear modification factor for central Au+Au collisions is compared to theoretical calculations that predict modifications of the direct photon yield due to initial state (IS) and final state (FS) effects [2–5]. IS effects include the isospin effect due to the different photon cross sections in $p+p$, $n+n$, and $p+n$ collisions (“Isospin effect” in Fig. 4), and modifications of nuclear structure functions due to shadowing and anti-shadowing (“EPS09 PDF”) [5]. The EPS09 calculation also includes the isospin effect.

FS modifications due to QGP lead, on one hand,

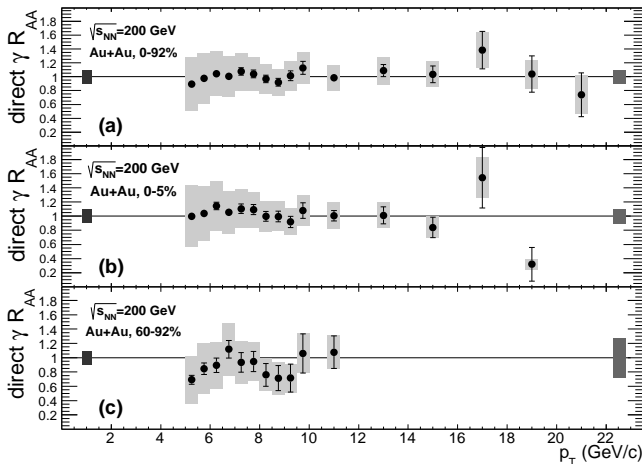


FIG. 3: Direct photon nuclear modification factor R_{AA} for three different centrality selections. The error bars show point-to-point uncertainties, the boxes around the points depict p_T correlated uncertainties. The boxes on the left show the uncertainty of the total inelastic $p+p$ cross section, the boxes on the right show the uncertainty in N_{coll} .

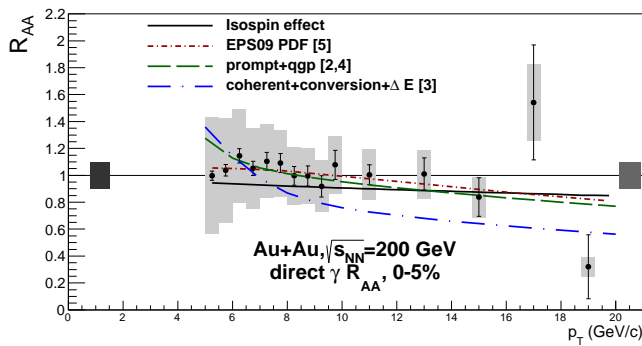


FIG. 4: Direct photon nuclear modification factor R_{AA} for 0 – 5% most central events, compared with theoretical calculations [2–5] for different scenarios. The boxes depict the same uncertainties as in Fig. 3. Note that the EPS09 curve is calculated for minimum bias collisions.

to a lower photon yield, since energy loss of a parton also means suppression of the corresponding fragmentation photon yield. On the other hand, QGP effects can increase the photon yield due to radiation resulting from jet-medium interactions (“prompt+QGP”) [2, 4]. This FS calculation also takes into account the aforementioned IS effects. Yet another calculation [3] includes IS effects, as well as FS energy loss and medium-induced photon bremsstrahlung and the LPM effect (“coherent+conversion+ ΔE ”). The data are consistent with a scenario where the hard scattered photons are produced taking account of the isospin effect and modifications of the nuclear PDFs and then simply traverse the matter unaffected. Balancing effects from the QGP such as fragmentation photon suppression and enhancement due to jet-medium interactions are not excluded by

the data. The approach in [3] is in disagreement with the data. This confirms that the majority (if not all) direct photons at high p_T come directly from hard scattering processes and suggests that possible effects from the QGP all but cancel.

In summary, PHENIX has measured direct photon spectra in Au+Au collisions at $\sqrt{s_{NN}} = 200$ GeV at midrapidity in the transverse momentum range of $4 < p_T < 20$ GeV/ c . The direct photon nuclear modification factor R_{AA} has been calculated as a function of p_T using a measured $p+p$ reference for the first time. It is consistent with unity for all centrality selections over the entire measured p_T range. Theoretical models for direct photon production in Au+Au collisions are compared to the data. Some of these models are found to be in quantitative agreement with the measurement while others appear to be disfavored by the data. Collectively, the effects of the QGP on the high p_T direct photon yield are apparently small.

We thank the staff of the Collider-Accelerator and Physics Departments at Brookhaven National Laboratory and the staff of the other PHENIX participating institutions for their vital contributions. We acknowledge support from the Office of Nuclear Physics in the Office of Science of the Department of Energy, the National Science Foundation, Abilene Christian University Research Council, Research Foundation of SUNY, and Dean of the College of Arts and Sciences, Vanderbilt University (U.S.A), Ministry of Education, Culture, Sports, Science, and Technology and the Japan Society for the Promotion of Science (Japan), Conselho Nacional de Desenvolvimento Científico e Tecnológico and Fundação de Amparo à Pesquisa do Estado de São Paulo (Brazil), Natural Science Foundation of China (P. R. China), Centre National de la Recherche Scientifique, Commissariat à l’Énergie Atomique, and Institut National de Physique Nucléaire et de Physique des Particules (France), Ministry of Industry, Science and Technologies, Bundesministerium für Bildung und Forschung, Deutscher Akademischer Austausch Dienst, and Alexander von Humboldt Stiftung (Germany), Hungarian National Science Fund, OTKA (Hungary), Department of Atomic Energy (India), Israel Science Foundation (Israel), National Research Foundation and WCU program of the Ministry Education Science and Technology (Korea), Ministry of Education and Science, Russian Academy of Sciences, Federal Agency of Atomic Energy (Russia), VR and the Wallenberg Foundation (Sweden), the U.S. Civilian Research and Development Foundation for the Independent States of the Former Soviet Union, the US-Hungarian NSF-OTKA-MTA, and the US-Israel Binational Science Foundation.

* Deceased

- [†] PHENIX Spokesperson: jacak@skipper.physics.sunysb.edu
- [1] R. J. Fries, B. Muller, and D. K. Srivastava, Phys. Rev. Lett. **90**, 132301 (2003).
- [2] S. Turbide, C. Gale, E. Frodermann, and U. Heinz, Phys. Rev. C **77**, 024909 (2008).
- [3] I. Vitev and B.-W. Zhang, Phys. Lett. B **669**, 337 (2008).
- [4] C. Gale, arXiv:0904.2184 (2009).
- [5] F. Arleo, K. J. Eskola, H. Paukkunen, and C. A. Salgado, JHEP **1104**, 055 (2011).
- [6] F. Arleo, JHEP **09**, 015 (2006).
- [7] K. Adcox et al. (PHENIX Collaboration), Phys. Rev. Lett. **88**, 022301 (2002).
- [8] S. Adler et al. (PHENIX Collaboration), Phys. Rev. Lett. **91**, 072301 (2003).
- [9] X.-N. Wang and M. Gyulassy, Phys. Rev. Lett. **68**, 1480 (1992).
- [10] S. S. Adler et al. (PHENIX Collaboration), Phys. Rev. Lett. **94**, 232301 (2005).
- [11] A. Adare et al. (PHENIX Collaboration), Phys. Rev. Lett. **104**, 132301 (2010).
- [12] K. Adcox et al. (PHENIX Collaboration), Nucl. Instrum. Meth. A **499**, 469 (2003).
- [13] M. L. Miller, K. Reygers, S. J. Sanders, and P. Steinberg, Annu. Rev. Nucl. Part. Sci. **57**, 205 (2007).
- [14] L. Aphecetche et al. (PHENIX Collaboration), Nucl. Instrum. Meth. A **499**, 521 (2003).
- [15] S. S. Adler et al. (PHENIX Collaboration), Phys. Rev. Lett. **98**, 012002 (2007).
- [16] *GEANT 3.2.1*, CERN Program Library (1993), <http://wwwasdoc.web.cern.ch/wwwasdoc/pdftdir/geant.pdf>.
- [17] A. Adare et al. (PHENIX Collaboration), Phys. Rev. Lett. **101**, 232301 (2008).
- [18] A. Adare et al. (PHENIX Collaboration), Phys. Rev. Lett. **C82**, 011902 (2010).
- [19] K. Nakamura et al. (Particle Data Group), J. Phys. G **37**, 075021 (2010).
- [20] A. Adare et al. (PHENIX Collaboration), arXiv:1205.5533 (2012), submitted to Phys. Rev. D.